Developing Effective Separation of Feldspar and Quartz While Recycling Tailwater by HF Pretreatment

Weiqing Wang [1], Jinyao Cong [1], Jie Deng [2], Xiaoqing Weng [3], Yiming Lin [1], Yang Huang [1] and Tiefeng Peng [1,*]

[1] Key Laboratory of Ministry of Education for Solid Waste Treatment and Resource Recycle, Southwest University of Science and Technology, Mianyang 621010, China; swustwwq@sohu.com (W.W.); congjinyao@126.com (J.C.); swustlym@163.com (Y.L.); swusthy@163.com (Y.H.)

[2] Research Center of Multipurpose Utilization of Metal Mineral Resources of China Geological Survey, Chengdu 610000, China; dengjie23@126.com

[3] School of Resource and Civil Engineering, Wuhan Institute of Technology, Wuhan 430073, China; zhaoxi1010@163.com

* Correspondence: pengtiefeng@cqu.edu.cn; Tel.: +86-816-6089438

Abstract: The effect of hydrofluoric acid (HF) pretreatment on flotation of feldspar and quartz using dodecylamine (DDA) as collector was investigated by micro-flotation, zeta potential, pyrene fluorescence spectroscopy, attenuated total reflection flourier transformed infrared spectroscopy (ATR-FTIR), scanning electron microscope (SEM), X-ray photoelectron spectroscopy (XPS) and bench scale flotation. The micro-flotation tests revealed that there was little difference in the flotation of feldspar and quartz at pH 2, using H_2SO_4 as pH regulator. After HF pretreatment, the floatability of feldspar significantly increased while the floatability of quartz showed no change. HF pretreatment resulted in leaching of SiO_2 and enrichment of Na, K and Al on the feldspar surface. Consequently, the negative surface charge of feldspar increased at pH 2, which allowed for the flotation separation of the feasible minerals. This took place via an increased electrostatic adsorption between DDA and Na, K, Al on the feldspar surface, which effectively increased its hydrophobicity and as a result, improved the floatability of feldspar. An alternative process which exhibited effective separation of quartz and feldspar while recycling the tailwater from the flotation was proposed.

Keywords: hydrofluoric acid; flotation; DDA; ATR-FTIR

1. Introduction

Feldspar minerals ($KAlSi_3O_8$, $NaAlSi_3O_8$, $CaAl_2Si_2O_8$) are the most abundant of aluminosilicate rock forming minerals, comprising 60% of the earth's crust. They are widely applied in the production of glass, ceramics, and as fillers and extenders [1,2] in the paper and paint industries. In order to improve the purity or the whiteness of feldspar, flotation [3–5] and magnetic separation are typically used to remove associated minerals (such as quartz, and dark-colored minerals rich in iron) from feldspar [6–8]. Traditionally, there are two main flotation separation processes to remove quartz from feldspar. The first one is hydrofluoric acid flotation, which uses hydrofluoric acid (HF) or fluoride (NaF) as a feldspar activator. Sulfuric acid (H_2SO_4) or hydrochloric acid (HCl) was used to adjust the flotation pulp in a strong acidic environment (pH = 2), and HF or NaF was added to activate the feldspar surface, and, finally, amine cationic was applied as a collector for the flotation separation of feldspar and quartz.

Previously, a selective flotation separation of feldspar in the presence of HF was proposed by Fuerstenau et al. [9] in an acidic environment (pH = 2.1). It was suggested that the HF method can

achieve a good separation of feldspar and quartz with a high grade of feldspar and a high-quality quartz [10]. However, there is a large amount of chemical activator (HF or NaF) in the flotation system, as the activator is added directly into the pulp. These fluoride ions are severely harmful to the surrounding environment. This will in turn increase production costs due to the treatment of flotation fluoride-containing tailwater, and limit the scope of this method in practical industrial application.

The second method is fluorine-free flotation, which could solve the problem caused by environmental pollution of HF flotation. Applying aliphatic amines and petroleum sulfonate mixing collector in strong acidic environment using H_2SO_4 or HCl as pH regulator, selective flotation separation of feldspar from quartz [11–13] could be achieved. However, the effectiveness of this separation method is worse than conventional fluorine-containing flotation. It can generally only obtain a product of quartz sand (or feldspar), and is not applicable on an industrial scale [14].

In the present work, the floatability of feldspar and quartz, both pure minerals and mineral mixtures, were comparatively investigated with or without HF pretreatment. The detailed mechanisms resulting from HF pretreatment were experimentally examined using various techniques, e.g., micro-flotation, zeta potential, pyrene fluorescence spectroscopy, ATR-FTIR, XPS and so on. The objective is to explore HF pretreatment on floatability of feldspar and quartz, to correlate these surface properties with that of flotation behavior difference. Moreover, an alternative method considering the above factors is to be developed, for effective separation of quartz and feldspar while recycling the tailwater.

2. Experimental

2.1. Materials and Reagents

The pure feldspar and quartz samples were hand-picked from the Lijiagou lithium mine of Jinchuan County, Sichuan province, China. After being crushed to size −2 mm and ground in an agate mortar, the X-ray diffraction (XRD) spectra of feldspar and quartz were examined and shown in Figure 1. The main mineral of the purified feldspar is shown to be Na-feldspar (pdf No. 80-1049), and the as-prepared pure quartz sample is α-SiO_2 (pdf No. 46-1045). Further chemical analysis showed that the quartz purity was 99.26%. The feldspar content was 95.42%, with oxide contents of 11.26% Na_2O, 0.32% K_2O, 18.95% Al_2O_3 and 69.03% SiO_2. The mineral samples were then wet-sieved to obtain size fractions of (−76 + 38 μm) and −38 μm. A portion of the −38 μm materials were further ground and micro-sieved in an ultrasonic bath to obtain a particle size of −2 μm. The coarse fraction (−76 + 38 μm) was used for micro-flotation and bench scale flotation tests, while the finer fraction (−2 μm) was for zeta potential, pyrene fluorescence spectroscopy, ATR-FTIR, SEM and XPS measurements.
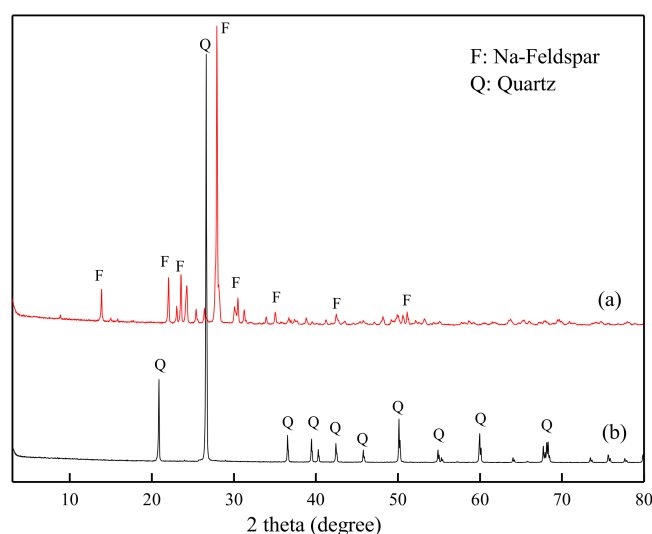
Figure 1. X-ray diffraction (XRD) spectra of the purified feldspar (a) and quartz (b).

The cationic diamine collector used was DDA, supplied by Aladdin Chemistry Co., Ltd., Shanghai, China. DDA was dissolved in dilute HCl. Analytical standard pyrene ($C_{16}H_{10}$) was used for pyrene fluorescence probe. Analytical grade HCl and sodium hydroxide (NaOH) were used for pH adjustment. The water used for all the experiments was deionized water with a resistivity of 18.3 M Ω cm.

2.2. HF Pretreatment

A portion of the $-76 + 38$ μm minerals were HF pretreated in an agitation froth machine in order to obtain HF pretreated pure minerals. The pulp density was 30%, stirring speed 1600 r/min, and stirring time 10 min. The pretreated minerals were then filtered, washed and dried at a temperature 150 °C to remove the fluorine ions. In order to examine the floatability of minerals, the $-76 + 38$ μm single fraction of feldspar and quartz, with and without HF pretreatment were studied by bench scale flotation tests.

2.3. Micro-Flotation Tests

The micro-flotation tests of the pure minerals were performed in a 40-mL hitch groove flotation cell, as a function of pH, HF concentration and collector concentration. The untreated or pretreated [15,16] pure mineral particles (2.0 g) were placed in a Plexiglas cell, and then filled with 35 mL deionized water. The pulp was continuously stirred for 2 min using a pH regulator (HCl or NaOH), and the collector (DDA) was added and agitated for another 3 min. Then, the pH of the suspension was recorded before flotation, and the flotation process [17,18] was conducted for 4 min. The concentrates were weighed after filtering and drying, and the mineral recovery was calculated. Each test (also for measurements, e.g., zeta potential) was measured no less than three times under the same experimental condition, and the mean value was taken as the final result, with the standard deviations as error bars.

2.4. Zeta Potential Measurements

The zeta potentials were measured using a Zetasizer Nano ZS90 (Malvern Instruments Ltd., Malvern, UK). The conductivity and pH of the suspension were monitored continuously during the measurement, and the environmental temperature was maintained at 25 °C. The suspension was prepared by adding 30 mg of the pure mineral fraction particles (-2 μm) to a glass bottle containing 50 mL deionized water, then, the glass bottle was placed into a thermostatic shaker (200 rpm) for 10 min. After settling for 10 min, the supernatant of the dilute fine particle suspension was obtained for zeta potential measurements.

2.5. Pyrene Fluorescence Probe

An ethanol solution of pyrene was prepared with 0.01 g pyrene and 100 mL ethanol in a beaker. The test suspensions were then prepared using 0.1 mL ethanol solution of pyrene, 2.0 g of the pure mineral particles (-2 μm), the test concentration of the pure collector, and 30 mL of ultra-pure water. The suspensions were then oscillated for 24 h using a constant temperature oscillator at room temperature (25 °C). The pyrene fluorescence spectra of the samples were obtained using a Perkin-Elmer LS55 fluorescence spectrophotometer (Perkin-Elmer, Waltham, MA, USA). The excitation wavelength of pyrene was 334 nm, and the width of the emission and excitation slits were 4 nm and 10 nm, respectively.

2.6. ATR-FTIR Measurements

The ATR-FTIR spectra were obtained by a Spectrum One (Version BM) FT-IR (Perkin-Elmer, Waltham, MA, USA), with a DTGS CsI detector in order to characterize the interaction between the collector and minerals. Samples were placed on a Ge crystal plate and scanned from 4000 to 600 cm^{-1} with resolution of 0.5 cm^{-1}. Each sample was scanned three times and identical spectra were obtained in each case. This process was done to verify the accuracy of the absorbance values. Average spectra were used for further analysis via OMNIC 8.0 software.

The suspension was prepared by adding 2.0 g of the untreated or pretreated pure mineral particles to 35 mL of ultra-pure water in a Plexiglas cell (40 mL). The pH of the suspension was adjusted by HCl or NaOH for 2 min, and then the suspension was conditioned for another 3 min with DDA. Finally, the solid samples were washed three times using ultra-pure water with the same pH. The washed samples for ATR-FTIR measurements were vacuum dried at 55 °C.

2.7. SEM and XPS Tests

SEM was utilized to visually examine the state of adsorption of feldspar and quartz using a Carl Zeiss AG-ULTRA 55 instrument (Oberkochen, Germany). The sample conditioning procedure was the same as that used for the micro-flotation tests. After conditioning, a pipette was applied to transfer a drop of the suspension to a ground slide, which was then examined under an electron microscope.

The XPS spectra were recorded on a Thermo Scientific Escalab 250Xi (Thermo Fisher, Waltham, MA, USA) photoelectron spectrometer under monochromatic Al Kα1 and Mg Kα1 X-ray radiation with sample cooling. Prior to analysis, the samples were out-gassed under vacuum for 72 h. The spectral resolution is 0.05 eV and the area of X-ray beam spots from 200 μm to 900 μm. Each analysis started with a survey scan from 0 to 1300 eV with a dwelling time of 8 s, and passing energy of 150 eV at steps of 1 eV with 1 sweep. For the high-resolution analysis, the number of sweeps was increased, the pass energy was lowered to 30 eV and the dwell time was changed to 0.5 s. The sample preparation was the same as that for ATR-FTIR measurements.

2.8. Bench Scale Flotation Tests

In order to verify the effect of HF pretreatment on the flotation separation [19] of feldspar and quartz, bench scale flotation tests were carried out using 300 g minerals in a laboratory flotation cell with a volume of 1 L. DDA collector (100 g/t) was added and conditioned further for 3 min, the pulp was then floated for 3 min. After the flotation of feldspar, the concentrates and tailings were filtered, washed and dried to analyze the flotation recovery of feldspar and quartz. The mass ratio of feldspar and quartz for bench scale flotation tests is 1:1.

3. Results and Discussion

3.1. Micro-Flotation

The flotation recovery of feldspar and quartz as a function of pH using DDA as collector (2.0×10^{-4} M) is shown in Figure 2. The recovery of feldspar and quartz increases with an increase in pH before HF pretreatment. The flotation recovery of feldspar is higher than that of quartz at the same pH when pH < 4, and the recovery of feldspar is still higher than that of quartz when pH > 4 (but the difference was narrowed). After HF pretreatment, and at pH < 2.5, the floatability of quartz showed little change while the floatability of feldspar increased substantially. This may be due to a partial dissolution of the feldspar surface as a result of HF pretreatment, which leads to an increased electrostatic adsorption of DDA at Al, Na, K sites. Vidyadhar et al. [11–13] demonstrated that feldspar can be selectively floated from quartz at pH 2, where the doubly positively charged collector species was adsorbed on the feldspar surface but not on the quartz surface.
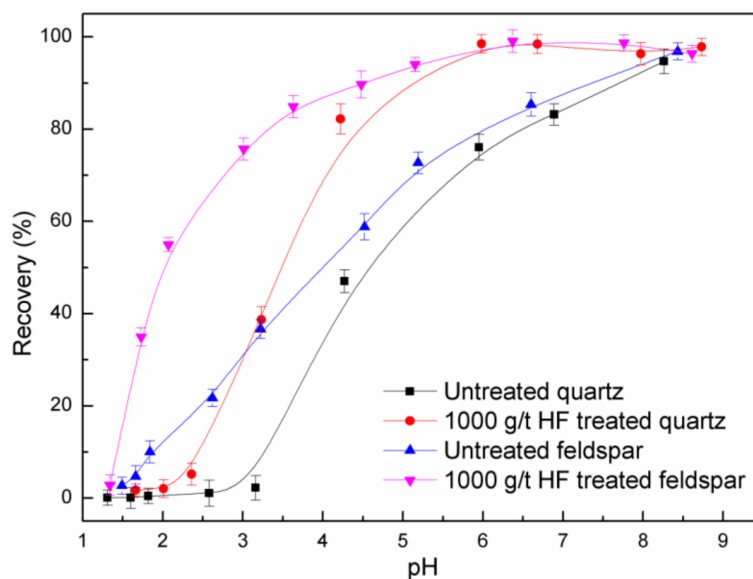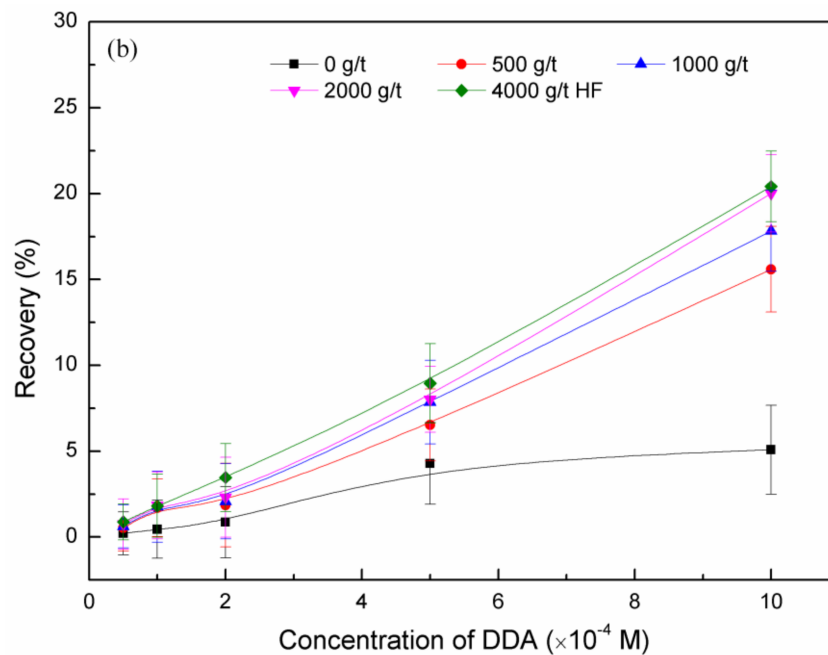
Figure 2. Flotation recovery of feldspar and quartz as a function of pH ($C_{DDA} = 2.0 \times 10^{-4}$ M).

The flotation recovery of feldspar and quartz at pH 2, as a function of concentrations of HF pretreatment and DDA, is shown in Figure 3. Under the same concentration of DDA, the flotation recovery of feldspar increased with HF pretreatment concentration. Under the same concentration of HF pretreatment, the floatability of feldspar increased with DDA concentration, and the flotation recovery did not increase further when the DDA concentration was ~5×10^{-4} M. Comparing the effect of HF pretreatment with that of non-treatment, the flotation recovery of quartz showed a smaller change than that of feldspar.
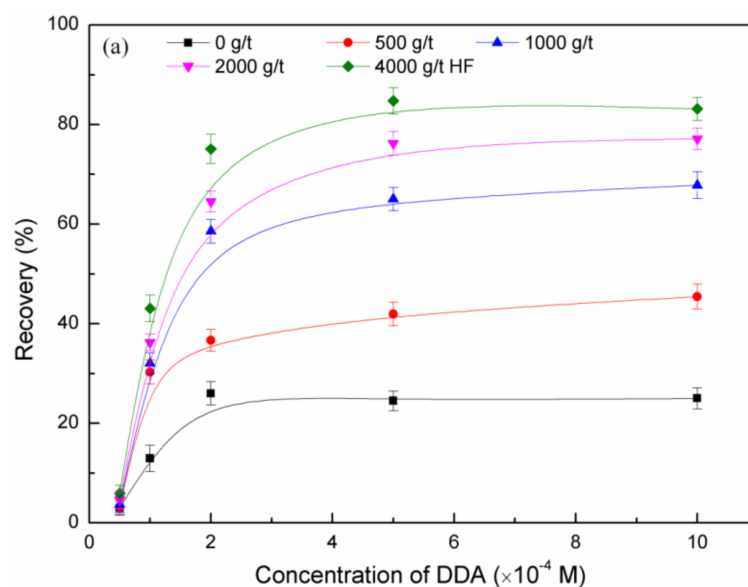

Figure 3. *Cont.*

Figure 3. Flotation recovery of feldspar (**a**) and quartz (**b**) as a function of dodecylamine (DDA) and hydrofluoric acid (HF) pretreatment.

3.2. Zeta Potential

The zeta potentials of feldspar and quartz, untreated and pretreated by HF (2000 g/t) with DDA (5×10^{-4} M) as a function of pH, are shown in Figure 4. The feldspar and quartz points of zero charge (PZC) are about pH 1.7 and 2.0, respectively [20]. In general, the PZC of feldspar minerals are reported at pH 1.5–2.0, and quartz had a slightly higher value. The feldspar surface exhibits negative charge while quartz possesses zero charge. The collector of DDA had a strong influence on the zeta potentials of both minerals. In the presence of DDA, the feldspar acquires increasing negative charge until about pH 3.0, and the zeta potentials increase with a charge reversal occurring at about pH 4.0.

The zeta potentials of quartz are less negative than in water solutions. After HF pretreatment, the zeta potentials of feldspar are more negative while the zeta potentials of quartz are less negative at pH 2.0 to 4.0. It could be explained with the fact that more negative charges facilitated the particle dispersion and thus enhanced the accessibility of DDA to feldspar, whereas the decreased charges of quartz lead to flocculation and agglomeration. These experimental measurements are consistent with the results of micro-flotation (Figures 2 and 3) that HF pretreatment has a more pronounced effect on increasing the floatability for feldspar.
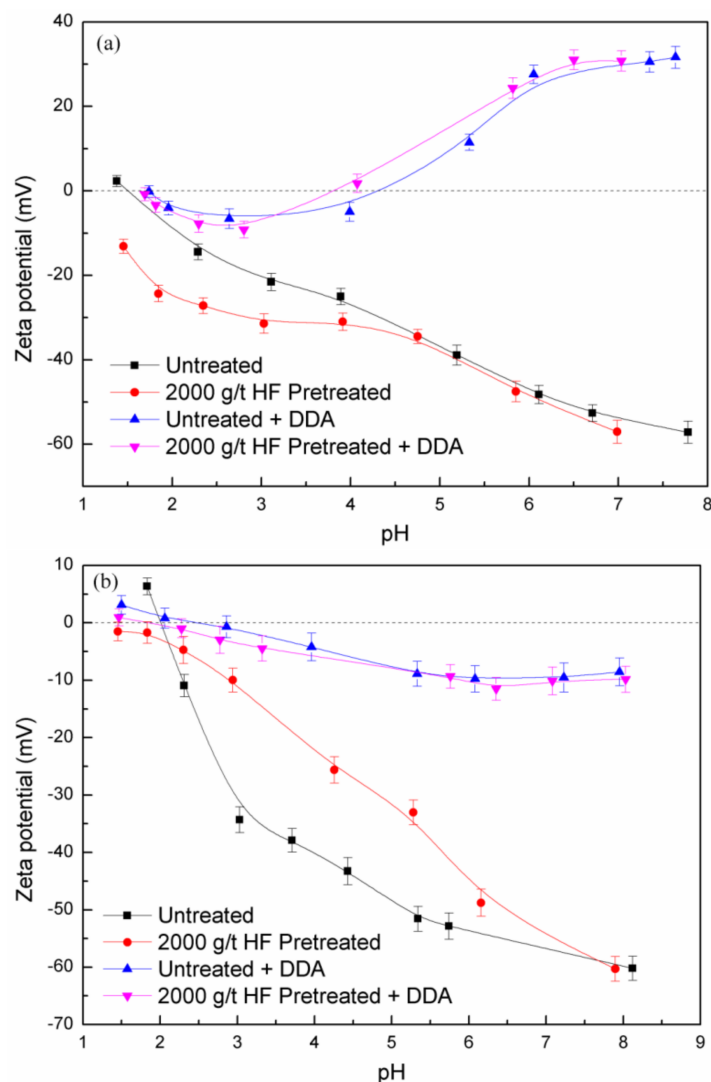
Figure 4. Zeta potentials of feldspar (**a**) and quartz (**b**) as a function of pH and HF pretreatment.

3.3. Pyrene Fluorescence Spectroscopy

Pyrene is a hydrophobic substance with strong fluorescence and is a good probe to study the surface adsorption mechanisms [21,22]. The typical emission spectrum of pyrene has five distinct peaks at 373, 379, 384, 390, and 397 nm [23]. The intensity ratio of the third and the first peaks (I_3/I_1) is sensitive to the solution environment of pyrene. The value of I_3/I_1 is 0.5–0.6 in a water environment, 0.8–0.9 in surfactant micelles environment, and >1 in non-polar solvents, respectively. This ratio decreases as the polarity increases, and, therefore, it can be used to estimate the solvent polarity of an unknown nano-environment in which the pyrene probe is located. Therefore, pyrene can be used as a fluorescent probe to study the "micro-polar" environment of the mineral surface and investigate the structure of the adsorbed layer of the collector [24]. The change in intensity ratio, I_3/I_1, of pyrene in DDA solutions at pH 2 is presented in Figure 5. The values of I_3/I_1 increased gradually as DDA concentrations increased. The values of I_3/I_1 changed sharply from 0.6, corresponding to pyrene in water, to about 1.09, corresponding to pyrene dissolved in collector's micelles. When the concentration was up to the critical micelle concentration (CMC), a flat horizontal was observed and I_3/I_1 reached its maximum value. The CMC for DDA is 2.0×10^{-3} M.

Figure 5 also shows the I_3/I_1 values for pyrene presence on the surfaces of untreated and pretreated minerals, as a function of the DDA concentration at pH 2. For untreated feldspar and

quartz, the I_3/I_1 values are less than 0.70 from 1.0×10^{-6} to 2.0×10^{-5} M DDA concentration (0.001–0.02 mM), and, therefore, the pyrene is in a polar environment. The I_3/I_1 value increased from 0.70 to 0.77, and the polar environment of pyrene became smaller with increasing DDA concentration from 2.0×10^{-5} to 5.0×10^{-4} M. When the DDA concentration was 5.0×10^{-3} M, the I_3/I_1 values on the feldspar and quartz surfaces were 0.84 and 0.75, respectively. This indicates that the feldspar surface in surfactant micelles environment while that of quartz is not. In other words, DDA is more easily adsorbed on the feldspar surface than quartz.

After HF pretreatment, the I_3/I_1 values on the feldspar and quartz surfaces showed little change, compared to the I_3/I_1 values for the untreated samples, in low concentration of DDA collector (1.0×10^{-6} to 2.0×10^{-4} M). The I_3/I_1 values on the feldspar and quartz surfaces increased sharply when the DDA concentration $>2.0 \times 10^{-4}$ M. When the DDA concentration reached 5.0×10^{-4} M, the feldspar surface would be in a surfactant micelles environment. The CMC for treated feldspar with DDA is 1.0×10^{-3} M, while for quartz treated feldspar with DDA it is about 2.0×10^{-3} M. The I_3/I_1 values of feldspar and quartz reached at the point of CMC are 0.98 and 0.95, respectively. This result indicates that the HF pretreatment has changed the "micro-polar" environment of the mineral surface by the reaction of selective dissolution.
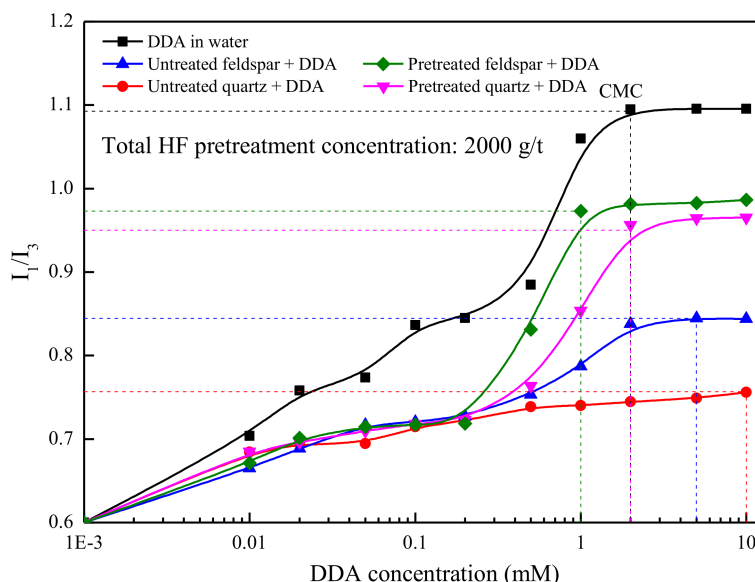
Figure 5. Values of I_3/I_1 on feldspar and quartz surface as a function of DDA concentration and HF pretreatment.

The observed changes in the I_3/I_1 value support the proposed mechanism of DDA activation on the mineral surface. At low concentrations, the cation surfactant would exist as a single ion that is adsorbed on the mineral surface through electrostatic attraction, and the polarity of the mineral surface is high. The adsorption capacity increased while the polarity of the mineral surface decreases with increasing cation surfactant concentration. When the I_3/I_1 value reached approximately 0.8, the cationic surfactant formed half micelles through the adsorption of hydrophobic association. The mineral surfaces are hydrophobic and this condition is favorable for flotation of feldspar.

3.4. ATR-FTIR Analysis of DDA Adsorption

The conventional FT-IR procedures require separating the mineral and collector solution followed by drying, grinding and preparing the sample in pellets. These are likely to cause changes in the microscopic state of the mineral surface, thus affecting the results [25]; however, ATR-FTIR could avoid these drawbacks. The ATR-FTIR spectra of feldspar, quartz and DDA in water environment are

presented in Figure 6. The ATR-FTIR spectra of quartz and feldspar, with or without HF pretreatment, at the presence of DDA (5×10^{-4} M) at pH 2 are shown in Figure 7.

In Figure 6, the bands at 3381 cm^{-1} and 1639 cm^{-1} are assigned to the stretching vibration absorption of –OH and bending vibration absorption of H_2O, respectively. In the ATR-FTIR spectra of feldspar, the bands at 1147 cm^{-1} and 1099 cm^{-1} are the stretching vibrations of Si–O. The stretching vibrations of Al–O are manifested by bands at 1035 cm^{-1} and 989 cm^{-1}. The band at 648 cm^{-1} corresponds to the bending vibration of O–Si–O [26]. In the ATR-FTIR spectra of quartz, the bands at 1088 cm^{-1} and 1061 cm^{-1} are the asymmetric stretching vibrations of Si–O, the bands at 773 cm^{-1} is the stretching vibration of Si–Si, and the bending vibration of O–Si–O is located at 681 cm^{-1} [27]. In the ATR-FTIR spectra of DDA, the bands corresponding to the stretching vibration of –CH$_2$– and to the bending vibration of –CH$_3$ are located at 2925 cm^{-1} and 2854 cm^{-1}, respectively [28]. The symmetric and asymmetric vibration absorption peaks of –NH$_2$ are located near 3400 cm^{-1}, overlap with the stretching vibration absorption peak of –OH, and are therefore not discernible.

The feldspar and quartz treated with DDA (untreated or pretreated with HF) (Figure 7) show weak stretching vibrations peaks belonging to the –CH$_3$ and –CH$_2$– group. The peaks associated with the stretching vibrations of Si–O did not change significantly. These results indicate that the feldspar and quartz surfaces have physical adsorption with DDA. The spectra of feldspar and quartz interacting with DDA after HF pretreatment show new stretching vibration absorption peaks of –CH$_3$ and –CH$_2$– at 2926 cm^{-1} and 2854 cm^{-1}. In addition, the peak assigned to the Si–O stretching vibrations of feldspar undergoes significant displacement (from 1147 cm^{-1} and 1099 cm^{-1}, to 1157 cm^{-1} and 1095 cm^{-1}, respectively). The peak assigned to the Si–O stretching vibrations of quartz undergoes a displacement from 1057 cm^{-1} to 1067 cm^{-1}. These results illustrate that the HF might have changed the surface Si–O structures after interacting with feldspar and quartz. The change of Si–O structure increases the negative charge and relative content of Na, K and Al surface elements of feldspar. When DDA cationic collector was added, the amine (RNH^{3+}) ions would be adsorbed [29] on the feldspar surface by electrostatic adsorption, and as a result the feldspar surface becomes hydrophobic. For feldspar by HF pretreatment, HF leaching Si–O lead to more active center Al^{3+} at the feldspar surface. For quartz, there was no selective acid corrosion on the surface by HF pretreatment due to the Si–O within the quartz structure. This was rooted and governed by their crystal structure differences.
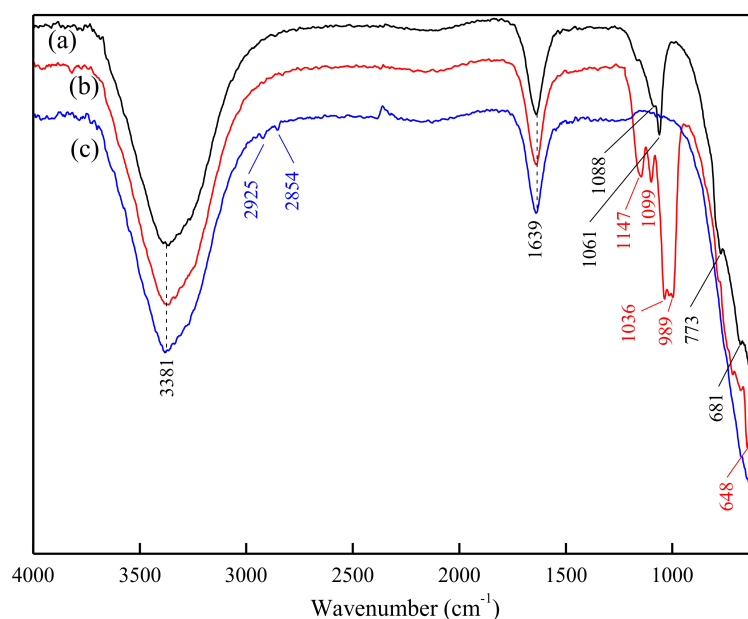

Figure 6. Attenuated total reflection flourier transformed infrared spectroscopy (ATR-FTIR) spectra of quartz (a), feldspar (b) and DDA (c) at pH 2 in water environment.
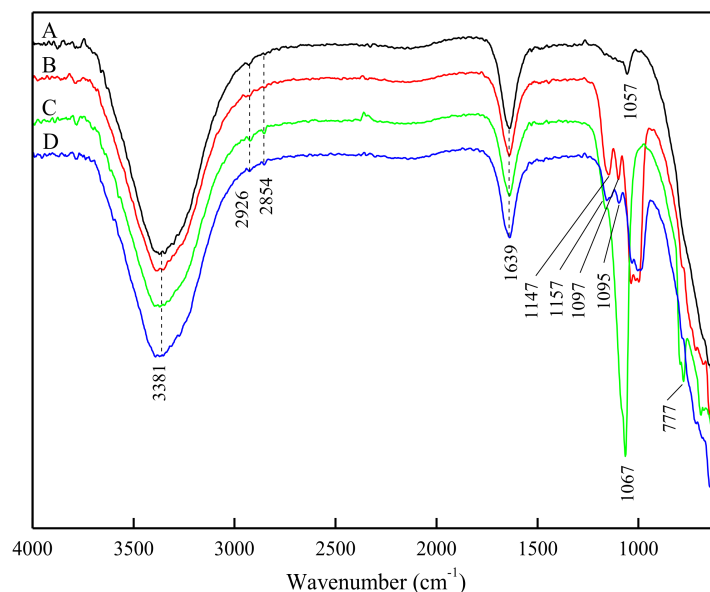
Figure 7. ATR-FTIR spectra of feldspar and quartz with DDA (5×10^{-4} M) at pH 2: (A) quartz and DDA, (B) feldspar and DDA, (C) pretreated quartz and DDA, and (D) pretreated feldspar and DDA.

3.5. SEM Patterns

In order to observe the change of micro topography of the minerals by HF, Figure 8 showed the SEM microphotographs of the minerals untreated and pretreated by HF (2000 g/t). The feldspar surface was flat and smooth before HF pretreatment, and uneven after HF pretreatment. The result illustrates that HF induced selective corrosion on the feldspar surface [30]. The feldspar surface exposed Al, Na and K, thus increasing the negative charge at pH = 2. This condition is favorable for adsorption of DDA on the feldspar surface. The quartz surface shows no obvious change. The phenomenon was consistent with the results of micro-flotation and zeta potential.
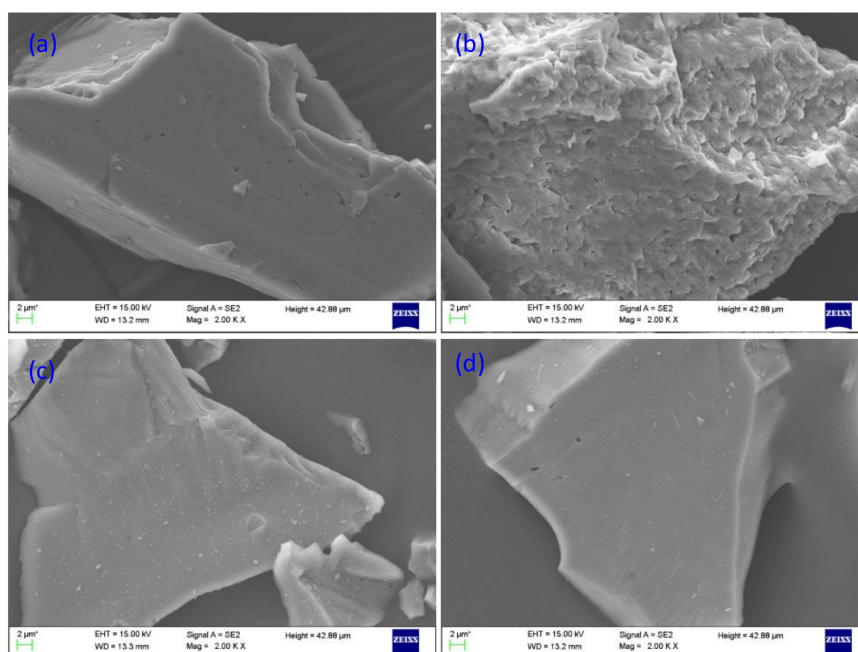

Figure 8. SEM microphotographs of untreated feldspar (**a**), HF pretreated feldspar (**b**), untreated quartz (**c**) and HF pretreated quartz (**d**).

3.6. XPS Analysis

It was inferred that DDA mainly interacts with Na, K and Al on the feldspar surface at pH 2 by ATR-FTIR analysis. To provide straightforward evidence of this, XPS measurements of feldspar and quartz were carried out, and are shown in Figure 9 (full spectrum scanning). The main peaks include: Al(2*p*) located at ~75 eV, Si(2*p*) at ~103 eV, C(1*s*) at ~285 eV, K(2*p*) at ~300 eV, O(1*s*) at ~531 eV, and Na(1*s*) at ~1072 eV [31–33]. The binding energy of elements on the mineral surfaces untreated and pretreated by 2000 g/t HF with 5×10^{-4} M DDA at pH 2 are listed in Table 1. The relative contents of elements are given in Table 2. In addition to the elements belonging to the mineral or the reagent, the presence of carbon, the so-called adventitious carbon, was observed on the minerals surface. According to the obtained results, the relative content of feldspar before HF pretreatment is mainly O, Al, Si, K and Na atoms.
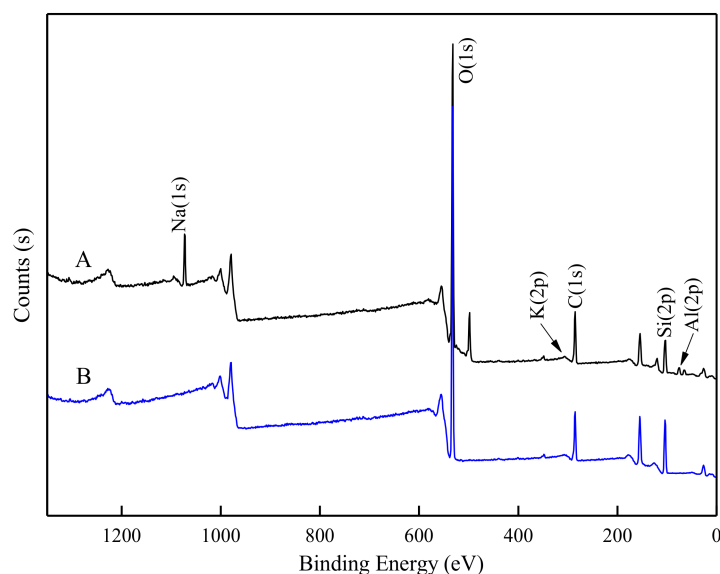
Figure 9. X-ray photoelectron spectroscopy (XPS) spectra of feldspar (A) and quartz (B).

Table 1. Binding energy of element on the surfaces of feldspar and quartz untreated and pretreated by 2000 g/t HF in DDA at pH 2.

Sample	Binding Energy (eV)						Chemical Shift (eV)					
	K(2*p*)	Na(1*s*)	Al(2*p*)	Si(2*p*)	O(1*s*)	C(1*s*)	K(2*p*)	Na(1*s*)	Al(2*p*)	Si(2*p*)	O(1*s*)	C(1*s*)
Untreated feldspar	299.3	1072.5	74.5	102.9	532.1	284.8	-	-	-	-	-	-
Pretreated feldspar	298.0	1072.4	74.4	102.8	532.0	284.8	−1.3	−0.1	−0.1	−0.1	−0.1	0.0
Pretreated feldspar + DDA	293.1	1068.8	74.2	102.7	528.3	284.8	−4.9	−3.6	−0.2	−0.1	−3.7	0.0
Untreated quartz	-	-	-	103.1	532.4	284.8	-	-	-	-	-	-
Pretreated quartz	-	-	-	103.1	532.3	284.8	-	-	-	−0.0	−0.1	0.0
Pretreated quartz + DDA	-	-	-	103.0	532.3	284.8	-	-	-	−0.1	−0.0	−0.0

Table 2. Relative content of elements on the surfaces of feldspar and quartz.

Sample	Surface Atomic Composition (%)						
	C	O	Si	Al	Na	K	N
Untreated feldspar	21.8	50.1	17.9	6.5	3.7	0.1	-
Pretreated feldspar	22.2	49.8	17.6	6.4	3.9	0.1	-
Pretreated feldspar + DDA	22.9	49.5	17.6	5.8	3.4	0.1	0.8
Untreated quartz	21.1	53.2	25.8	-	-	-	-
Pretreated quartz	21.1	53.0	26.0	-	-	-	-
Pretreated quartz + DDA	22.6	51.5	25.2	-	-	-	0.7

The content of the elements O and Si atoms on the feldspar surface decreases as that of the Na and K atoms increases, which indicates that HF pretreatment damages the Si–O surface structure and leads to an enrichment of Na and K atoms of the feldspar surface. After interacting with DDA, the XPS spectra of feldspar and quartz show the presence of N(III). The relative contents of N are 0.8% and 0.7%, respectively.

After HF pretreatment of feldspar, the binding energies of K(2p), Na(1s), Al(2p), Si(2p) and O(1s) shift −1.3 eV, −0.1 eV, −0.1 eV, −0.1 eV and −0.1 eV, respectively. The result revealed that a chemical interaction occurred between the F ion and K, Na, Al, Si atoms on the feldspar surface. After interacting with DDA, the binding energies of K(2p), Na(1s), Al(2p), Si(2p) and O(1s) shift −4.9 eV, −3.6 eV, −0.2 eV, −0.1 eV and −3.7 eV, respectively. Such changes suggest that chemical interaction existed between DDA and K, Na, Al and O atoms on the feldspar surface. However, the binding energies of the elements in the quartz sample treated by HF with DDA showed little changes.

3.7. Effective Separation of Quartz and Feldspar

The results of micro-flotation tests (Figures 2 and 3) indicate that a selective feldspar flotation from quartz using mineral fractions with coarse particle size seems feasible. Furthermore, bench scale flotation tests (Table 3) were performed in order to compare the floatability of various mineral mixtures with and without HF pretreatment and to verify the advantages of the proposed process (Figure 10).
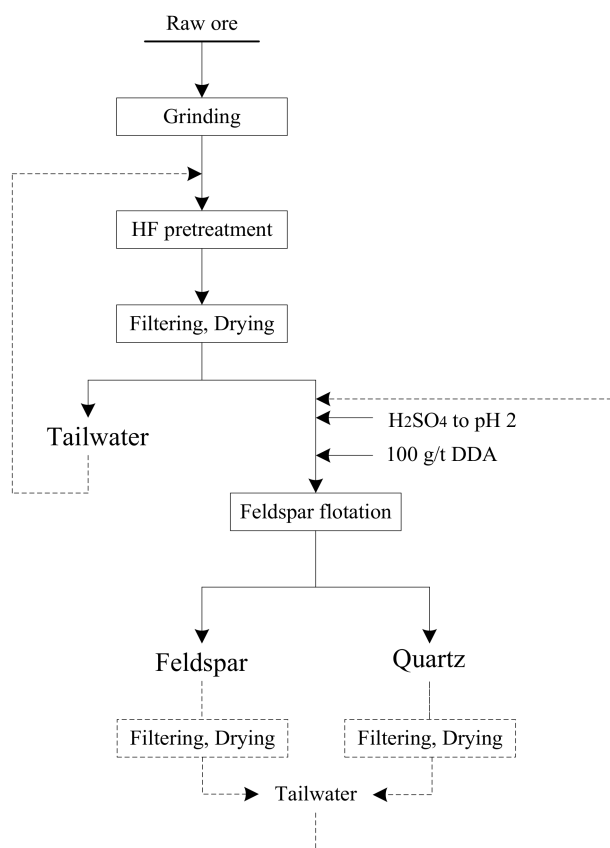
Figure 10. Proposed process for effective separation of quartz and feldspar while recycling the tailwater from flotation.

The results from flotation tests show that the Na$_2$O and K$_2$O grade of the feldspar concentrate is 10.24% and 0.29% after HF pretreatment, respectively. Meanwhile, the HF pretreatment can separate the feldspar and quartz at pH 2. The remaining feldspar can be separated by repeatedly sweeping to obtain a high-quality quartz concentrate. The method of HF pretreatment can effectively separate

the feldspar from quart, the tailwater of HF pretreatment can then be recycled, and treatment of the tailwater containing H_2SO_4 and DDA is feasible.

To the best of our knowledge, this method has not been reported, and the advantages are that: (1) the wastewater of solid-liquid separation contains fluoride ions and other inorganic ions (such as Fe, K, Na) by only pretreatment, therefore it is easy to deal with; (2) tailwater from feldspar and quartz flotation does not contain fluoride ions, thus it can be reused [34].

Table 3. Flotation results of artificial mixture of feldspar and quartz using DDA as collector.

Flotation Technology	Products	Yield (%)	Grade (%)			Recovery (%)		
			Na$_2$O	K$_2$O	SiO$_2$	Na$_2$O	K$_2$O	SiO$_2$
Untreated	Concentrate	10.94	7.83	0.32	78.64	15.21	21.92	10.15
	Tailing	89.06	5.36	0.14	85.48	84.79	78.08	89.85
	Feed	100.00	5.63	0.16	84.73	100.00	100.00	100.00
Pretreated by HF (2000 g/t)	Concentrate	50.79	10.24	0.29	72.26	92.39	90.89	43.32
	Tailing	49.21	0.87	0.03	97.6	7.61	9.11	56.68
	Feed	100.00	5.63	0.16	84.51	100.00	100.00	100.00

4. Conclusions

There is little difference in the flotation of natural feldspar and quartz at pH 2. After HF pretreatment, the floatability of feldspar increases with an increase of HF concentration and DDA concentration, while the floatability of quartz shows little change. The zeta potentials show that HF pretreatment can increase the negative charges on the feldspar surface, resulting in an expected increase in DDA adsorption with a concomitant increase in the flotation recovery. Subsequent pyrene fluorescence spectroscopy of these minerals in the presence of DDA collector show that the mineral surfaces switch from polar to non-polar. The results of ATR-FTIR indicate a substantial change of the feldspar and quartz surfaces structures due to reaction with HF. This is confirmed by the change of morphology after HF pretreatment by SEM. The XPS analysis shows that the binding energies of K(2p), Na(1s), Al(2p) and O(1s) on the feldspar surface undergo shifts, while there is little change for the quartz surface, which confirms that a chemical interaction between DDA and feldspar occurred. An effective separation of quartz and feldspar while recycling the tailwater was established based on bench scale flotation tests.

Author Contributions: Weiqing Wang and Tiefeng Peng conceived and designed the experiments; Weiqing Wang, Jinyao Cong, Jie Deng, Xiaoqing Weng, Yiming Lin, Yang Huang performed the experiments; Weiqing Wang and Tiefeng Peng analyzed the data; Weiqing Wang and Tiefeng Peng wrote the paper.

Conflicts of Interest: The authors declare no conflict of interest.

References

1. Abdel-Khalek, N.A.; Yehia, A.; Ibrahim, S.S. Technical note beneficiation of egyptian feldspar for application in the glass and ceramics industries. *Miner. Eng.* **1994**, *7*, 1193–1201. [CrossRef]
2. Wu, J.-F.; Li, Z.; Huang, Y.-Q.; Li, F.; Yang, Q.-R. Fabrication and characterization of low temperature co-fired cordierite glass–ceramics from potassium feldspar. *J. Alloys Compd.* **2014**, *583*, 248–253. [CrossRef]
3. Basnayaka, L.; Subasinghe, N.; Albijanic, B. Influence of clays on the slurry rheology and flotation of a pyritic gold ore. *Appl. Clay Sci.* **2017**, *136*, 230–238. [CrossRef]
4. Han, J.; Jiao, F.; Liu, W.; Qin, W.; Xu, T.; Xue, K.; Zhang, T. Innovative methodology for comprehensive utilization of spent MgO-Cr$_2$O$_3$ bricks: Copper flotation. *ACS Sustain. Chem. Eng.* **2016**, *4*, 5503–5510. [CrossRef]

5. Xia, W.; Zhou, C.; Peng, Y. Enhancing flotation cleaning of intruded coal dry-ground with heavy oil. *J. Clean. Prod.* **2017**, *161*, 591–597. [CrossRef]

6. Elshall, H.; Vidanage, S.; Somasundaran, P. Grinding of quartz in amine solutions. *Int. J. Miner. Process.* **1979**, *6*, 105–121. [CrossRef]

7. Scott, J.L.; Smith, R.W. Diamine flotation of quartz. *Miner. Eng.* **1991**, *4*, 141–150. [CrossRef]

8. Vieira, A.M.; Peres, A.E.C. The effect of amine type, pH, and size range in the flotation of quartz. *Miner. Eng.* **2007**, *20*, 1008–1013. [CrossRef]

9. Fuerstenau, D.W.; Raghavan, S. The crystal chemistry, surface properties and flotation behaviour of silicate minerals. *Proc. XII Int. Miner. Process. Congr.* **1977**, *2*, 368–415.

10. Hanumantha Rao, K.; Forssberg, K.S.E. Mixed collector systems in flotation. *Int. J. Miner. Process.* **1997**, *51*, 67–79. [CrossRef]

11. Shehu, N.; Spaziani, E. Separation of feldspar from quartz using edta as modifier. *Miner. Eng.* **1999**, *12*, 1393–1397. [CrossRef]

12. Vidyadhar, A.; Hanumantha Rao, K.; Chernyshova, I.V.; Pradip; Forssberg, K.S.E. Mechanisms of amine–quartz interaction in the absence and presence of alcohols studied by spectroscopic methods. *J. Colloid Interface Sci.* **2002**, *256*, 59–72. [CrossRef]

13. Vidyadhar, A.; Hanumantha Rao, K.; Chernyshova, I.V. Mechanisms of amine–feldspar interaction in the absence and presence of alcohols studied by spectroscopic methods. *Colloids Surf. A Physicochem. Eng. Asp.* **2003**, *214*, 127–142. [CrossRef]

14. Sekulic, Z.; Canic, N.; Bartulovic, Z.; Dakovic, A. Application of different collectors in the flotation concentration of feldspar, mica and quartz sand. *Miner. Eng.* **2004**, *17*, 77–80. [CrossRef]

15. Thanh Truc, N.T.; Lee, B.-K. Combining ZnO/microwave treatment for changing wettability of WEEE styrene plastics (ABS and HIPS) and their selective separation by froth flotation. *Appl. Surf. Sci.* **2017**, *420*, 746–752. [CrossRef]

16. Cao, S.; Cao, Y.; Liao, Y.; Ma, Z. Depression mechanism of strontium ions in bastnaesite flotation with salicylhydroxamic acid as collector. *Minerals* **2018**, *8*, 66. [CrossRef]

17. Zhao, Q.; Liu, W.; Wei, D.; Wang, W.; Cui, B.; Liu, W. Effect of copper ions on the flotation separation of chalcopyrite and molybdenite using sodium sulfide as a depressant. *Miner. Eng.* **2018**, *115*, 44–52. [CrossRef]

18. Zhang, X.; Zhu, Y.; Xie, Y.; Shang, Y.; Zheng, G. A novel macromolecular depressant for reverse flotation: Synthesis and depressing mechanism in the separation of hematite and quartz. *Sep. Purif. Technol.* **2017**, *186*, 175–181. [CrossRef]

19. Chen, W.; Feng, Q.; Zhang, G.; Li, L.; Jin, S. Effect of energy input on flocculation process and flotation performance of fine scheelite using sodium oleate. *Miner. Eng.* **2017**, *112*, 27–35. [CrossRef]

20. Fuerstenau, D.W.; Pradip. Zeta potentials in the flotation of oxide and silicate minerals. *Adv. Colloid Interface Sci.* **2005**, *114–115*, 9–26. [CrossRef] [PubMed]

21. Baldi, L.D.C.; Iamazaki, E.T.; Atvars, T.D.Z. Evaluation of the polarity of polyamide surfaces using the fluorescence emission of pyrene. *Dyes Pigment.* **2008**, *76*, 669–676. [CrossRef]

22. Arunima, C.; Sourav, H.; Amitabha, C. Organization and dynamics in micellar structural transition monitored by pyrene fluorescence. *Biochem. Biophys. Res. Commun.* **2009**, *390*, 728–732.

23. Zhang, J.; Wang, W.-Q.; Liu, J.; Huang, Y.; Feng, Q.-M.; Zhao, H. Fe(III) as an activator for the flotation of spodumene, albite, and quartz minerals. *Miner. Eng.* **2014**, *61*, 16–22.

24. Li, L.; Hao, H.; Yuan, Z.; Liu, J. Molecular dynamics simulation of siderite-hematite-quartz flotation with sodium oleate. *Appl. Surf. Sci.* **2017**, *419*, 557–563. [CrossRef]

25. Wijnja, H.; Schulthess, C.P. ATR-FTIR and DRIFT spectroscopy of carbonate species at the aged γ-Al$_2$O$_3$/water interface. *Spectrochim. Acta Part A* **1999**, *55*, 861–872. [CrossRef]

26. Xu, H.; van Deventer, J.S.J. The effect of alkali metals on the formation of geopolymeric gels from alkali-feldspars. *Colloids Surf. A Physicochem. Eng. Asp.* **2003**, *216*, 27–44. [CrossRef]

27. Wang, Y.-H.; Ren, J.-W. The flotation of quartz from iron minerals with a combined quaternary ammonium salt. *Int. J. Miner. Process.* **2005**, *77*, 116–122.

28. Wang, L.; Sun, W.; Hu, Y.-H.; Xu, L.-H. Adsorption mechanism of mixed anionic/cationic collectors in muscovite- quartz flotation system. *Miner. Eng.* **2014**, *64*, 44–50. [CrossRef]

29. Long, X.; Chen, J.; Chen, Y. Adsorption of ethyl xanthate on ZnS(110) surface in the presence of water molecules: A DFT study. *Appl. Surf. Sci.* **2016**, *370*, 11–18. [CrossRef]

30. Hu, P.; Zhang, Y.; Huang, J.; Liu, T.; Yuan, Y.; Xue, N. Eco-friendly leaching and separation of vanadium over iron impurity from vanadium-bearing shale using oxalic acid as a leachant. *ACS Sustain. Chem. Eng.* **2018**, *6*, 1900–1908. [CrossRef]

31. Yin, W.Z.; Sun, C.Y. X-ray photoelectron spectrometric analysis on surface property of silicate minerals. *J. Northeast. Univ. (Nat. Sci.)* **2002**, *23*, 156–159.

32. Shchukarev, A.; Sjöberg, S. XPS with fast-frozen samples: A renewed approach to study the real mineral/solution interface. *Surf. Sci.* **2005**, *584*, 106–112. [CrossRef]

33. Baer, D.R.; Gaspar, D.J.; Nachimuthu, P.; Techane, S.D.; Castner, D.G. Application of surface chemical analysis tools for characterization of nanoparticles. *Anal. Bioanal. Chem.* **2010**, *396*, 983–1002. [CrossRef] [PubMed]

34. Dorfner, S.; Trindle, H.; Jakobs, U. Electrostatic feldspar quartz separation without hydrofluoric acid reduces pollution. *Dev. Miner. Process.* **2000**, *13*, 30–33.